A Concentration-Dependent Mechanism by which Serum Albumin Inactivates Replacement Lung Surfactants

H. E. Warriner,* J. Ding,* A. J. Waring,[†] and J. A. Zasadzinski*

*Department of Chemical Engineering, University of California, Santa Barbara, California 93106 and [†]Department of Pediatrics, Harbor/UCLA Medical Center, Torrance, California 90502 USA

ABSTRACT   Endogenous lung surfactant, and lung surfactant replacements used to treat respiratory distress syndrome, can be inactivated during lung edema, most likely by serum proteins. Serum albumin shows a concentration-dependent surface pressure that can exceed the respreading pressure of collapsed monolayers in vitro. Under these conditions, the collapsed surfactant monolayer can not respread to cover the interface, leading to higher minimum surface tensions and alterations in isotherms and morphology. This is an unusual example of a blocked phase transition (collapsed to monolayer form) inhibiting bioactivity. The concentration-dependent surface activity of other common surfactant inhibitors including fibrinogen and lysolipids correlates well with their effectiveness as inhibitors. These results show that respreading pressure may be as important as the minimum surface tension in the design of replacement surfactants for respiratory distress syndrome.

INTRODUCTION

Human lung surfactant (LS) is a complex mixture of lipids and proteins that forms a monolayer at the alveolar liquid-air interface. This monolayer modulates the surface tension of the lung, lowering the normal air-water surface tension of ~70 mN/m to near zero on expiration, thereby stabilizing alveoli against collapse during expiration and minimizing the work of expanding the alveolar surface during inhalation (Goerke, 1998). Lack of effective surfactant in premature infants results in neonatal respiratory distress syndrome (NRDS), a potentially fatal disorder characterized by reduced lung compliance and oxygenation (Spragg et al., 1987). Transbronchial application of replacement LS (RLS) preparations has proven a beneficial treatment, significantly reducing mortality rates (Robertson, 1987; Gunther et al., 1998). Currently, the most effective RLS come from animal sources, but concern over potential viral contamination, adverse immunological responses, and the limited supply of animal surfactant (Spragg et al., 1987) drives continuing research in synthetic RLS formulations.

Acute respiratory distress syndrome (ARDS), which affects adults and children, has an incidence of 150,000 cases per year in the United States and a mortality rate of ~50% (Hyers, 1991). ARDS has a more complicated pathology than the simple absence of surfactant, but shares many NRDS symptoms, such as diminished lung compliance, marked restriction of lung volumes, and profound hypoxemia largely attributable to shunting of blood past unventilated lung units. Hence, it was hoped ARDS might respond favorably to RLS therapy. However, clinical trials with the most effective formulations used in NRDS yield gains in ARDS patients that are both modest and transient (Spragg, 1991; Hyers, 1991; McIntyre et al., 2000). Extracted bronchial fluid (lavage) from ARDS patients consistently shows elevated levels of serum proteins (Spragg, 1991; Nakos et al., 1998), and the ratio of soluble protein to LS in lavage correlates with severity and outcome in both NRDS and ARDS (Hallman et al., 1987). ARDS lavage also has a markedly reduced surface activity both in terms of the speed with which it adsorbs to an exposed air-water interface and the minimum surface tension achieved (Spragg, 1991). Biophysical studies of LS deliberately mixed with serum proteins show that, at sufficiently high protein concentrations, ARDS-like depression of RLS surface activity can be obtained. Centrifugation, which removes contaminating cells and proteins, restores normal surface activity in vitro (Holm et al., 1985).

These observations suggest that serum proteins in the lung can be a significant factor in the development of ARDS. As serum proteins inactivate both endogenous and replacement LS, serum proteins likely reduce RLS efficacy in NRDS (Spragg, 1991). Unfortunately, the mechanism of serum protein inhibition has remained obscure, frustrating efforts to rationally construct RLS formulations appropriate for ARDS. Current treatment consists of increased frequency and dosage of surfactants designed for use with NRDS, a regimen largely based on in vitro work showing that an increased ratio of RLS to inhibitor protein favors the competitive adsorption of RLS to the air-water interface (Holm et al., 1990; Holm et al., 1999). However, to date this therapy is no more successful than traditional RLS (Spragg and Smith, 1998; McIntyre et al., 2000). Delivering the amount of surfactant suggested for ARDS treatment by the in vitro experiments may be difficult to achieve in practice, especially in adults. For instance, Spragg (1987) suggested that an expected adult dose of 50–200 mg/kg body weight would require ~23 h to deliver by aerosol. Other authors have put the optimal therapeutic dose even higher, in the

range of 200–800 mg/kg body weight (Gunther et al., 1998).

RLSs consist primarily (>98% by weight) of dipalmitoylphosphatidylcholine (DPPC), unsaturated phosphatidylcholines and phosphatidylglycerols, fatty acids, and cholesterol. There are often small fractions ($\leq$ 2 wt%) of two surfactant specific proteins, SP-B and SP-C (Tanaka et al., 1986; Mizuno et al., 1995; Goerke, 1998). SP-B and SP-C are difficult to isolate from natural sources, so most commercial RLS formulations contain significantly lower amounts of protein than do native surfactants (Spragg and Smith, 1998; Mizuno et al., 1995). The composition of the model surfactant used in this study is a simplified version of the lipid composition of the clinically used RLS, beractant (Survanta, Ross Products, Columbus, OH): 69% (w/w) DPPC, 21% palmitoyl oleoyl phosphatidylglycerol (POPG), and 10% palmitic acid (PA). However, there is a wide variation in lipid and protein content between the various replacement and native surfactants; the optimal LS composition has not yet been established (Bernhard et al., 2000).

We present Langmuir isotherms and fluorescence micrographs showing that albumin concentrations above 0.1 mg/ml generate a surface pressure that exceeds the pressure at which an overcompressed, or "collapsed" model RLS monolayer reverts to the monolayer form or "respreads." Preventing respreading inhibits the control of interfacial tension; surprisingly, it also disrupts the monolayer structure. This inhibition mechanism is independent of molecular details; it arises solely from the concentration-dependent surface activity of albumin and should therefore be applicable to any other surface-active molecule. Indeed, in vivo and in vitro inhibition by lysolipids and two other serum proteins, immunoglobulin (Ig)G and fibrinogen, correlates with their concentration-dependent surface activity (Holm et al., 1999). Hence, the respreading pressure should become an important consideration in the design of replacement surfactants for respiratory distress syndrome.

MATERIALS AND METHODS

The Langmuir trough was milled from a solid piece of Teflon (DuPont, Wilmington, DE) with a working surface area of ~120 cm^2 and a subphase volume of ~150 ml (Lipp et al., 1997). A single Teflon barrier runs linearly along the top edge of the trough and is driven by a motorized translation stage. The barrier is spring-loaded against the trough and the ends of the barrier in contact with the well edges are beveled at an angle of ~10° to minimize leakage of surfactant. Temperature control of the subphase is achieved through the use of nine thermoelectric cooling elements. The trough can be operated over a temperature range of 10–50°C. A simple feedback loop allows for measurement and control of the subphase temperature. Expansion and compression speeds ranged from quasistatic (~30–60 min per expansion/compression cycle) to the maximum speed available in our trough (~30 s/cycle); no significant variations in the isotherms were observed over these cycle times. A Wilhelmy plate pressure sensor with a filter paper plate (R&K, Wiesbaden, Germany) was calibrated before each experiment using the liquid expanded-liquid condensed (LE-LC) kink of palmitic acid at 25°C (Peterson et al., 1992).

DPPC, POPG, and PA were purchased from Avanti Polar Lipids (Alabaster, AL) and were used as received. Monolayers were made by mixing 69 w/w% DPPC, 21 w/w % POPG, and 10 w/w% PA in a ~1-mg/ml chloroform (Fisher Spectranalyzed) solution and spreading onto a 25°C buffered subphase (pH 7 ($\pm$ 0.2), 150 mM NaCl, 2.0 mM CaCl$_2$, 0.2 mM NaHCO$_3$) in the Langmuir trough. The lipid mixture was doped with 0.5–1 mol% of the fluorescent lipid Texas red 1,2-dihexadecandyl-sn-glycero-3-phosphoethandamine (DHPE) (Molecular Probes, Eugene, OR) to enable simultaneous fluorescence imaging and isotherms. The fluorescent probe segregates to disordered or fluid phases, which then appear bright in images; the probe is absent from the solid or liquid condensed phases, which appear black or dark (Knobler and Desai, 1992). Similar data taken at 37 $\pm$ 0.5°C showed that the isotherms and morphologies were essentially independent of temperature over this range.

For the experiments incorporating albumin in the subphase, 5.1 ml of buffer was withdrawn from the subphase and 5.1 ml of a 50.8-mg/ml bovine serum albumin (BSA) in buffer was injected beneath the collapsed RLS monolayer. The barrier was stopped throughout injection and mixing of the albumin. The final subphase concentration was 2.0 mg/ml BSA doped with 2.2 w/w % napthenol-blue BSA (Molecular Probes) to permit visual verification of subphase homogeneity. The RLS monolayer was held well above the equilibrium spreading pressure of albumin during injection and a 20-min post-injection mixing.

For fluorescence imaging, a Nikon Optiphot (Tokyo, Japan) with the stage removed is positioned above the trough. Either a 5 or 40X power long working distance objective designed for use with fluorescence systems is used. The trough is mounted on a motorized xyz translation stage: the z axis is used for focusing and the x and y axes are used to scan over different regions. A 100-watt high-pressure mercury lamp was used for excitation. A dichroic mirror/barrier filter assembly is used to direct the excitation light onto the monolayer (with a normal angle of incidence) and to filter the emitted fluorescence. The emitted fluorescence is collected by the objective and detected via a silicon intensified target camera (Dage-MTI, Michigan City, IN). Images are recorded by a JVC (Yokohama, Japan) super-VHS videocassette recorder and digitized via a Scion (Frederick, MD) frame grabber.

RESULTS

Successive isotherms of this model RLS mixture (Fig. 1) illustrate two crucial properties of an effective LS: a high surface pressure at monolayer collapse and good retention of material at the interface after collapse. To minimize the work of breathing, an effective LS must have a high collapse pressure (low minimum surface tension); this RLS lipid mixture has a collapse pressure of 68 $\pm$ 3 dyn/cm ($n = 20$), close to the theoretical limit of 72 dyn/cm at 25°C. Measurements within the alveoli of excised animal lungs at functional residual capacity found a surface pressure of 63–67 dyn/cm (Schürch et al., 1976, 1978), similar to the collapse pressure of our model LS (Fig. 1). At collapse, surfactant is forced from the monolayer into the subphase with no further increase in the surface pressure (Fig. 1 B), producing a plateau in the isotherm (Fig. 1 B on isotherm) and the formation of multilayer folds in the monolayer (Lipp et al., 1998).

Whether this collapsed material is lost to the subphase or is drawn back onto the interface during expansion is crucial to surfactant performance (Notter, 2000). LS monolayers reside at the alveolar interface for hundreds of breathing
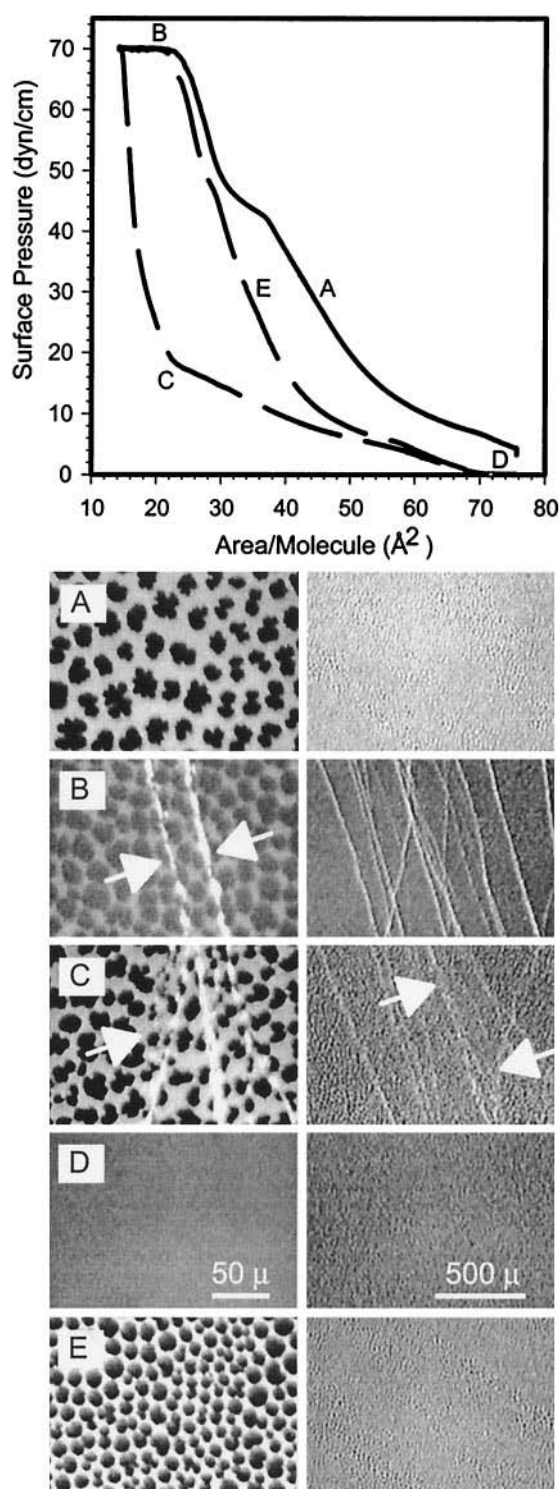
FIGURE 1 Two successive surface pressure, π, versus area per molecule isotherms and corresponding fluorescence micrographs for the model RLS composed of 69 w/w% DPPC, 21 w/w % POPG, 10 w/w% PA on a 25°C buffered subphase (pH 7 ($\pm$ 0.2), 150 mM NaCl, 2.0 mM CaCl$_2$, 0.2 mM NaHCO$_3$) in a custom-built Langmuir trough (Lipp et al., 1997). Similar isotherms and images taken at 37°C showed that the monolayer phase behavior was essentially independent of temperature over this range. Labels A–E on the images refer to surface pressures on the isotherm. Images were taken at two different magnifications at each surface pressure (left

cycles before replacement (Pison et al., 1996). Surfactant respreading from the collapse structures to the useful monolayer may be estimated by comparing the onset area of collapse in successive isotherms (Notter, 2000); for this lipid mixture, the apparent recovery of the collapsed material is quite high, 88 $\pm$ 6% ($n = 17$). The actual recovery is likely higher as the small lipid fraction lost is most likely because of leakage around the trough barriers at high surface pressure. Fluorescence images of the RLS monolayer at various points along the isotherm show the progression of structural features. At 30 dyn/cm (A on isotherm) during the compression limb of the cycle (Fig. 1 A, two magnifications) there is a bright, continuous network separating dark, flower-like structures. The bright network consists of a fluid- or liquid-expanded phase to which most of the fluorescent dye segregates (McConnell, 1991), whereas the dark domains are semicrystalline (Bringezu et al., 2001; Lipp et al., 1998; Knobler and Desai, 1992). This morphology seems to be the key to the desirable collapse properties of RLS. The condensed-phase domains resist compression, yielding a high collapse pressure, whereas the fluid network allows the monolayer to fold continuously into a surface-associated multilayer phase that can be drawn back onto the interface during expansion. This large-scale buckling can be seen in the bright lines crisscrossing the RLS monolayer at collapse (Lipp et al., 1998; Diamant et al., 2000) (Fig. 1 B, arrows). Similar collapse structures have been observed in the clinical surfactant Survanta (Ding et al., 2001). Nearly identical isotherms and morphologies were observed at 37°C, showing that the monolayer phase behavior was essentially independent of temperature over this range.

Monolayer collapse is a first-order phase transition and can be highly hysteretic. Thus, the multilayer folds in these model RLS (Fig. 1 B) do not immediately return to the monolayer when the surface pressure drops below the col-

column is higher magnification). The first compression-expansion cycle in the isotherm is denoted by the solid curve, the second with a dashed line. (A) At a surface pressure of 32 dyn/cm the characteristic morphology is of a bright, liquid-expanded phase network surrounding dark, liquid-condensed domains. (B) At the "collapse pressure" of 68 $\pm$ 3 dyn/cm ($n = 20$) the RLS can not maintain the monolayer structure and begins to buckle into surface-associated multilayers, resulting in the bright lines in the micrograph. The fraction of this overcompressed material drawn back onto the interface during expansion defines the percentage recoverability (%R). For this mixture, each cycle is only slightly offset from the previous, indicating that most material returns to the interface; in a set of 17 trials, an average of 88 $\pm$ 6% of the overcompressed material was recovered per cycle. Most of the material is lost because of leakage around the trough barriers at this low surface tension. Recovery begins when the collapse structures revert back to the monolayer form of RLS. (C) The collapse structures begin to convert to the monolayer when the surface pressure drops below ~15 dyn/cm; the last bright line finally disappears at ~5 dyn/cm. (D) Further expansion leads to a uniform liquid-expanded phase. (E) Upon recompression, the monolayer reorganizes back into the network morphology (A) and the cycle repeats.

lapse pressure. In the initial phase of expansion, collapse lines move apart but do not disappear, indicating that the monolayer spreads without reincorporating the multilayer material. In fact, reincorporation of the collapsed material begins (Fig. 1 *C*, arrows) only after the surface pressure falls below 15–20 dyn/cm. This appears as a sudden change in the slope of the isotherm (Fig. 1 *C*). However, the last collapse structures do not disappear until ~5 dyn/cm. At this surface pressure, the monolayer reverts to a uniform, disordered state (Fig. 1 *D*). Upon recompression, the monolayer reorganizes into the characteristic fluid-network morphology and the cycle repeats (Fig. 1 *E*).

When 2.0 mg/ml albumin is added to the subphase, however, RLS activity is dramatically altered. Fig. 2 *A* shows two compression-expansion cycles. At the end of the collapse plateau of the first cycle (Fig. 2 *A*), the barrier was stopped and sufficient albumin was injected and stirred beneath the monolayer to achieve a subphase concentration of 2.0 mg/ml. On expansion, the minimum surface pressure of the monolayer was 14 dyn/cm (Fig. 2, *A–C*), approximately equal to the maximum surface pressure of a 2-mg/ml albumin solution (Fig. 5). Recompressing the monolayer produced the same collapse pressure but no overlap between the two isotherms (Fig. 2, *A–D*). That is, the fraction of collapsed material that returned to the monolayer dropped from 90 to 0%.

The longer-term effects of albumin on RLS activity demonstrate that this material loss is not through solubilization. Fig. 2 *B* shows the maximum surface pressures achieved during 6 h of RLS cycling on subphases with albumin concentrations ranging from 0 to 2 mg/ml. Even for the most concentrated albumin subphases, the maximum surface pressure remains the same for several hours, indicating that a significant fraction of the surfactant monolayer remains at the interface. Solubilization, if it occurs, is extremely gradual and is unable to account for the 50% loss of the monolayer in the 40 min between points A and D in Fig. 2 *A*. Moreover, because collapse pressure is a sensitive function of composition (Notter, 2000), the stability of the pressure maximum argues against selective solubilization of a particular RLS component.

In fact, fluorescence micrographs clearly show that albumin acts by preventing the multilayer to monolayer transition upon expansion of the interface. The collapse folds and surrounding monolayer are unchanged by the processes of injection and mixing (postmixing photos in Fig. 3 *A*). However, now these multilayers remain intact up to the very limits of trough expansion (Fig. 3 *B*), indicating that albumin interferes with the respreading mechanism of RLS. In the next compression, the network structure begins to distort, especially near collapse structures persisting from the previous cycle (Fig. 3 *C*). On the second cycle, new multilayer folds form at the collapse pressure. These appear distorted compared with first cycle collapse structures (Fig. 3 *D*, left and right column). After more than 12 h of cycling,
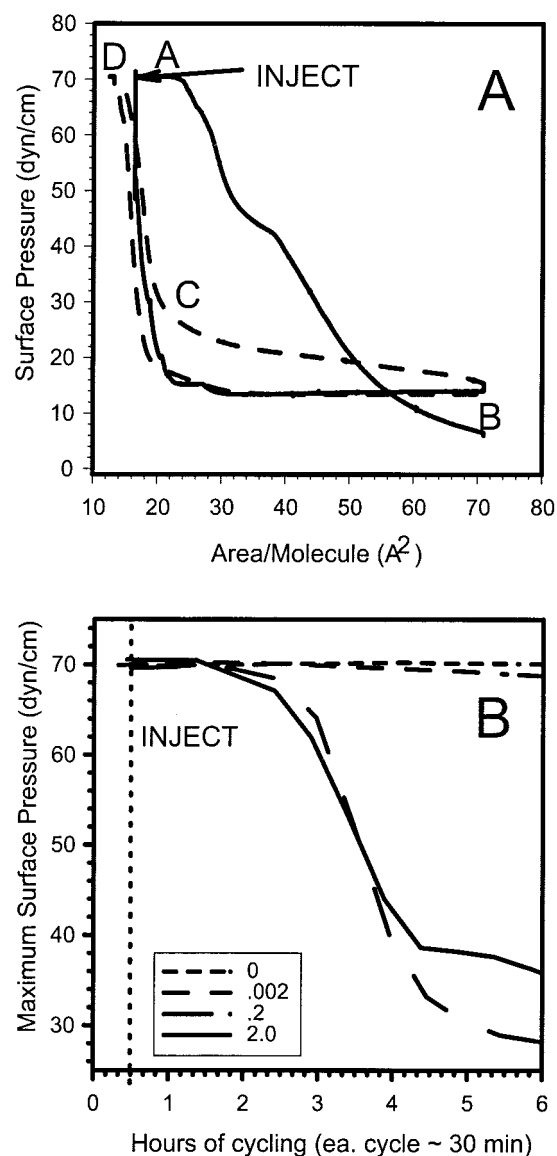

FIGURE 2 (*A*) Isotherms and (*B*) maximum surface pressure vs. elapsed time for the model RLS composed of 69 w/w% DPPC, 21 w/w % POPG, 10 w/w% PA on a 25°C buffered subphase before and after injection of BSA. (*A*) The first cycle is denoted by the solid line, the second (postinjection) by the dotted line. The cycles show no overlap of the collapse plateau (points A, D), indicating that no material returns to the interface during the expansion of the interface after injection of albumin. The lowest surface pressure obtained at maximum trough expansion increases from 0 without albumin (Fig. 1) to >14 dyn/cm (*B*). (*B*) Surface pressure at minimum trough area for the RLS monolayer for 6 h after injection; subphase albumin concentrations range from 0 to 2 mg/ml. Speed of area dilation was 0.096 cm^2/s for all cycles; each cycle took ~30 min. Note that all concentrations require at least 2–3 h to significantly lower maximum surface pressure. Because the impact is also not proportional to albumin concentration (0.2 and 2 mg/ml show the same effect), it is clear that solubilization is not important.

the network morphology (Fig. 1 *A*) has completely disappeared, but collapsed multilayers are still detectable (Fig. 3 *E*). As the collapsed structures are unable to modify inter-
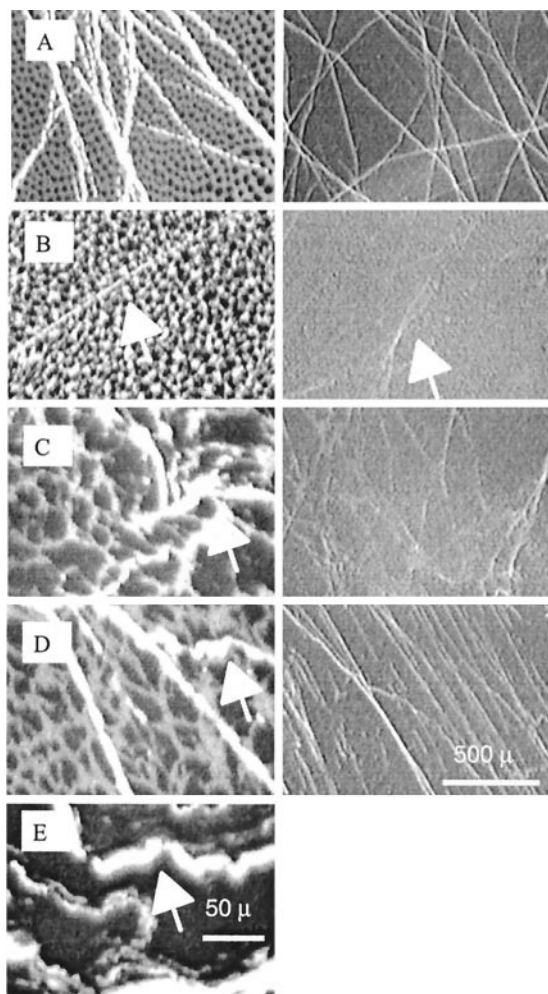
FIGURE 3 Fluorescence micrographs for the model RLS on a 25°C buffered subphase before and after injection of BSA to a final concentration of 2 mg/ml. Labels *A–D* correspond to points in the isotherm of Fig. 2 *A*. (*A*) Immediately after injection and mixing of albumin into the subphase, the monolayer retains the network morphology typical of RLS monolayers and similar collapse structures. (*B*) Collapse structures move apart during expansion but do not release the overcompressed material even at maximum trough area (*arrows*). In the absence of albumin, these collapse structures begin to reincorporate their material during expansion. (*C*) During the compression limb of the second cycle, the characteristic network morphology begins to distort. This distortion is especially evident near collapse structures persisting from the first cycle (*arrows*). (*D*) Newly forming collapse folds appear more disordered and fragmented (*arrows*) compared with collapse structures without albumin (Fig. 1) at both high and low magnification. (*E*) After 12 h of cycling, the network morphology has completely disappeared, but collapsed structures are clearly visible (*arrows*).

facial tension, normal surfactant function is eventually lost as is observed in vivo and in vitro.

The major features of inhibition can be reproduced on an albumin-free subphase simply by not allowing the RLS monolayer to reach the multilayer to monolayer transition pressure, as shown in Fig. 4. During the initial compression, the monolayer formed the characteristic network structure

(Fig. 4 *A*) and collapsed normally (Fig. 4 *B*). The interface was then expanded only far enough to allow the surface pressure to decrease to 15 dyn/cm and maintained at that pressure. After 20 min, collapse structures were still clearly visible and the monolayer network structure showed distortion (Fig. 4 *C*) similar to that on albumin-containing subphases (cf. Fig. 3 *C*). Distortion increased during recompression and collapse (Fig. 4 *D*), and there was no overlap between the first and second collapse plateaus (just as observed when albumin fixed the minimum surface pressure). Normal monolayer appearance (Fig. 4 *E*) and bioactivity are restored (overlap of green and black plateaus in isotherm) only when the monolayer was fully expanded so that the multilayer-monolayer transition pressure is reached.

Inhibition is known to be strongly dependent on both the species and concentration of inhibitor (Holm et al., 1990; Fuchimukai et al., 1987). In Fig. 5, surface pressures of fibrinogen, albumin, and IgG, three proteins commonly implicated in surfactant inhibition, are given as a function of concentration. The equilibrium surface pressure exerted by a surface-active, soluble protein (or any other species) is a logarithmic function of bulk concentration up to a certain bulk concentration at which the surface becomes saturated (Hiemenz, 1986). From Fig. 5, albumin and fibrinogen concentrations 0.1 mg/ml and greater exert surface pressures exceeding RLS respreading pressure, whereas IgG requires 100 times that concentration to reach similar pressures. Thus, albumin and fibrinogen should not inhibit much below 0.1 mg/ml, and IgG should have little effect until 1 mg/ml or more. This prediction agrees well with our experiments on albumin (Fig. 2 *B*) and with classic work (Seeger et al., 1985) establishing the relative inhibitory capacity of several serum proteins. In that work, albumin and fibrinogen were shown to be potent inhibitors requiring concentrations of just 0.1 and 0.01 mg/ml, respectively, whereas IgG had little effect even at 1 mg/ml. This relationship between inhibitory power and surface activity seems to hold for nonprotein inhibitors as well. For lysopalmitoylphosphatidylcholine, the surface pressure at the surface saturation concentration of 0.004 mg/ml is 34 mN/m (Yamanaka et al., 1997), significantly above the monolayer respreading pressure of 15 mN/m. Holm et al. (1999) showed that lysophosphatidylcholine is a more potent inhibitor than albumin, which requires a minimum concentration of 0.1 mg/m to reach a surface pressure of 15 mN/m.

DISCUSSION

LS isotherms are generally characterized by a significant hysteresis between the compression and expansion cycles (Goerke, 1998). One cause of this hysteresis is the formation of three-dimensional structures at the maximum or "collapse" surface pressure on compression (Fig. 1 *B*), which revert back to the monolayer at a significantly lower respreading pressure on expansion (Fig. 1 *C*). For the model
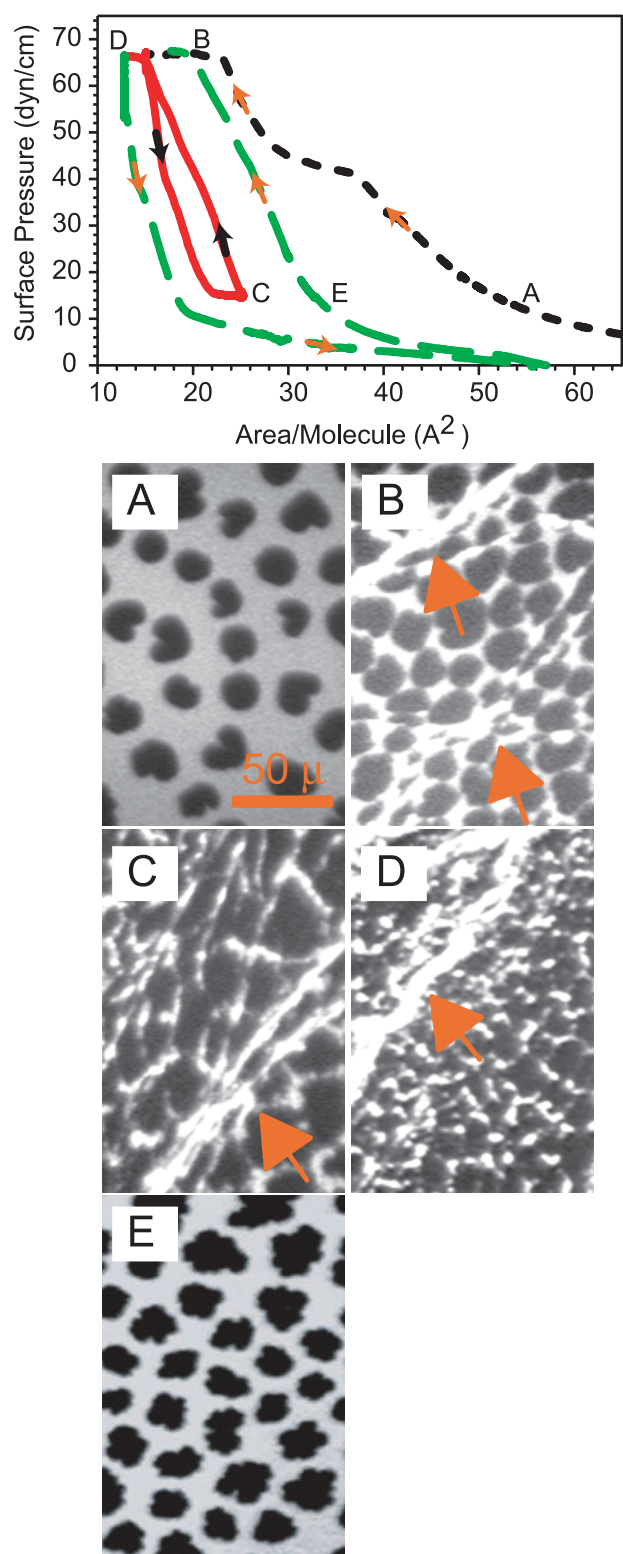
surfactant mixtures examined here, the collapse pressures were ~70 mN/m, whereas respreading began at 15–20 mN/m. If any other surface-active component is present at sufficient concentration that its surface pressure exceeds the respreading pressure of the monolayer, the transition from the collapse structure to the monolayer is inhibited (Fig. 3 *E*). Albumin, fibrinogen, and lysolecithin are sufficiently surface active that their surface pressure reaches 15–20 mN/m at physiologically relevant concentrations. Eventually, this inhibition causes more and more monolayer material to be trapped in the collapse structures, and the ability of the monolayer to lower surface tension is compromised (Fig. 3 *E*).

However, relating the minimum surface pressure necessary for respreading in vitro collapse structures to in vivo lung function is complicated. The minimum *static* surface pressure within excised lungs was measured to be ~40 mN/m (surface tension of ~30 mN/m) (Bachofen et al., 1987; Schürch et al., 1976, 1978), whereas the equilibrium spreading pressure of natural and replacement surfactants varies from 10–40 mN/m (Goerke, 1998; Schürch et al., 1976, 1978). To our knowledge, in vivo measurements of dynamic alveolar surface tension during respiration have yet to be performed, so the true range of surface pressures obtained during breathing is unknown. In our experiments, we dealt solely with monolayers spread from solvents with no surfactant present in the subphase. Future experiments should show if competitive adsorption of surfactant present in the subphase will lead to a sufficient increase in the respreading pressure to allow the collapse structures to reincorporate into the monolayer even in the presence of serum proteins.

The change in surface area of the lungs during breathing is an important corollary to the range of surface tension during breathing. When lung volume changes from 40 to 100% of total lung capacity, the lung epithelial cell basal surface area increases 35% (Tschumperlin and Margulies, 1999). However, the actual area change of the air-fluid

FIGURE 4 Successive isotherms and fluorescence micrographs for the model RLS on a 25°C buffered subphase. The monolayer is first compressed to collapse (*black dotted line*); however, in contrast to Fig. 1, the expansion is controlled so that surface pressure drops back to 15 dyn/cm and maintained at that pressure for 20 min before recompression to the same collapse pressure (*red line*). The monolayer is then fully expanded to a surface pressure of zero and again compressed to collapse (*green dotted*

line). Labels *A–E* in the isotherm identify the images. (*A*) In the initial compression, the characteristic morphology of a bright, liquid-expanded phase network surrounding dark, condensed domains is seen at moderate pressure. (*B*) The monolayer collapses at the expected pressure, forming surface-associated multilayers. (*C*) After ~30% overcompression, the monolayer is expanded until the surface pressure drops to 15 dyn/cm. After 20 min at 15 dyn/cm, the collapse cracks remain but the network morphology appears twisted and distorted, especially in the vicinity of cracks. (*D*) This distortion worsens as the monolayer is recompressed to collapse. In the isotherm, the new collapse plateau shows no overlap with the first collapse plateau, confirming that the material sequestered in the collapse structures in the first cycle is unavailable to subsequent cycles. Thus, isotherms and images obtained on clean buffer with artificially elevated surface pressure reproduce the essential features of isotherms and images on a concentrated albumin subphase (Figs. 2 *A* and 3). (*E*) Fully expanding the monolayer, which releases the material sequestered in the collapse structures, restores morphology in the next compression normally.
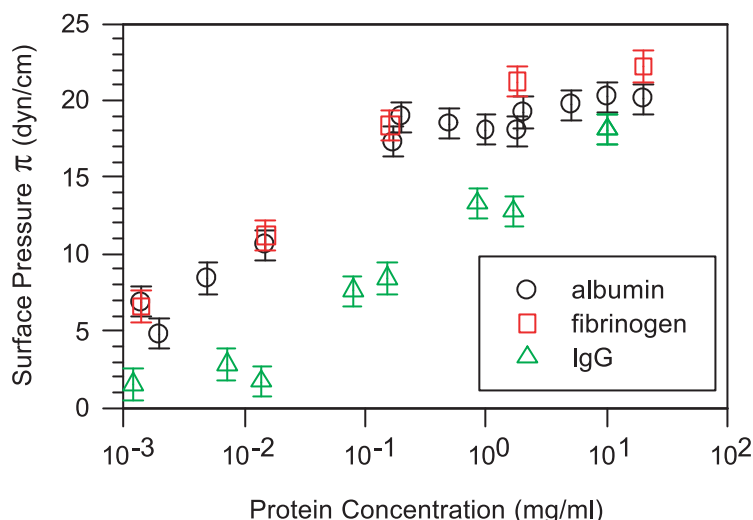
FIGURE 5 Surface pressure π vs. protein concentration for bovine albumin, fibrinogen, and IgG at $25 \pm 1°C$ in 150 mM NaCl, 2.0 mM $CaCl_2$, 0.2mM $NaHCO_3$ (pH 7 ± 0.2) buffer. Measurement error was estimated at ± 1.0 dyn/cm for both tensiometers. Fibrinogen and albumin exert a higher surface pressure than IgG at all concentrations measured. Near 0.1 mg/ml fibrinogen and albumin exert pressures exceeding the respreading pressure of collapsed LS, whereas IgG requires >1 mg/ml. The minimum concentration necessary to reach the spreading pressure of the RLS monolayer correlates well with in vivo inhibition by these serum proteins.

interface is more difficult to measure (Wirtz and Dobbs, 2000). The change in relative area in Langmuir isotherms is arbitrary; the monolayer area can be changed sufficiently so that the entire range between the collapse pressure and zero surface pressure is recorded. The relative change in surface pressure for a given change in area is typically much greater on expansion than on compression of the monolayer (See Figs. 1, 2, 4), especially after monolayer collapse. Hence, a given change in area could result in a much larger change in surface pressure depending on the history of the monolayer. It is unclear if the change in surface area during normal breathing would cause the collapse structures to occur or disappear on each breathing cycle. Our observation that in vitro surfactant recovery requires an area expansion sufficient to reduce the surface pressure below 15–20 mN/m is consistent with classic experiments by Mead and Collier (1959) showing that diminished lung compliance caused by mechanical ventilation with low and invariant tidal volumes could be normalized by a single large inflation of the lungs. Secretion of surfactant from the Type II cell is postulated to be induced by deep sighing breaths and the resulting large increases in lung surface area (Wirtz and Dobbs, 2000); similar deep breaths could result in elimination of the collapse structures in favor of monolayers as shown in Fig. 4.

The correlation between inhibitor surface activity and degree of inhibition may prove to be general, i.e., that concentration-dependent surface activity can be used as a reliable predictor of inhibitory potential. It is unclear what governs the respreading pressure of a particular surfactant mixture. For instance, the LS proteins SP-B and SP-C affect monolayer morphology and collapse and thus may have a significant effect on respreading (Lipp et al., 1998; Ding et

al., 2001). However, our results show that the respreading pressure of RLS should be an important design criterion in developing new surfactants to resist inhibition. Altering the surface activity of inhibitors by reducing inhibitor concentrations below the threshold concentration predicted by surfactant respreading pressure or by chemically altering inhibitor surface activity (Taeusch et al., 1999) might also prove beneficial in eliminating inhibition.

REFERENCES

Bachofen, H., S. Schürch, M. Urbinelli, and E. R. Weibel. 1987. Relations among alveolar surface tension, surface area, volume and recoil pressure. *J. Appl. Physiol.* 62:1878–1887.

Bernhard, W., J. Mottaghian, A. Gebert, G. A. Rau, H. von der Hardt, and C. F. Poets. 2000. Commerical versus native surfactants. *Am. J. Crit. Care Med.* 162:1524–1533.

Bringezu, F., J. Q. Ding, G. Brezesinski, and J. A. Zasadzinski. 2001. Changes in model lung surfactant monolayers induced by palmitic acid. *Langmuir.* 17:4641–4648.

Diamant, H., T. Witten, A. Gopal, and K. Y. Lee. 2000. Unstable topography of biphasic surfactant monolayers. *Eur. Phys. Lett.* 52:171–177.

Ding, J. Q., D. Y. Takamoto, A. von Nahmen, M. M. Lipp, K. Y. Lee, A. J. Waring, and J. A. Zasadzinski. 2001. Effects of lung surfactant proteins, SP-B and SP-C, and palmitic acid on monolayer stability. *Biophys. J.* 80:2262–2272.

Fuchimukai, T., T. Fujiwara, A. Takahashi, and G. Enhorning. 1987. Artificial pulmonary surfactant inhibited by proteins. *J. Appl. Physiol.* 62:429–437.

Goerke, J. 1998. Pulmonary surfactant: functions and molecular composition. *Biochim. Biophys. Acta.* 1408:79–89.

Gunther, A., D. Walmrath, R. Grimminger, and W. Seeger. 1998. Alteration of pulmonary surfactant in ARDS–pathogenetic role and therapeutic perspectives. *In* Acute Respiratory Distress Syndrome: Cellular and Molecular Mechanisms and Clinical Management. S. Matalon, J. I. Sznajder, and N. A. Division, editors. Plenum Press, New York. 97–106.

Hallman, M., J. L. Abraham, O. Pitkanen, and Arjomaa. 1987. Diagnosis of surfactant defects in newborn, children and adults in the era of surfactant therapy. *In* International Symposium on Surfactant Replacement Therapy. B. Lachmann, editor. Springer-Verlag, Rotterdam, Netherlands.58–65.

Hiemenz, P. C. 1986. Principles of Colloid and Surface Chemistry. Marcel Dekker, Inc., New York.

Holm, B. A., R. H. Notter, and J. N. Finkelstein. 1985. Surface property changes from interactions of albumin with natural lung surfactant and extracted lung lipids. *Chem. Phys. Lipid.* 38:287–298.

Holm, B. A., A. R. Venkitaraman, G. Enhorning, and R. H. Notter. 1990. Biophysical inhibition of synthetic lung surfactants. *Chem. Phys. Lipid.* 52:243–250.

Holm, B. A., Z. Wang, and R. H. Notter. 1999. Multiple mechanisms of lung surfactant inhibition. *Pediatr. Res.* 46:85–93.

Hyers, T. M. 1991. Adult respiratory distress syndrome: definition, risk factors and outcome. *In* Adult Respiratory Distress Syndrome. W. M. Zapol and F. Lemaire, editors. Marcel Dekker, New York. 23–33.

Knobler, C. M., and R. C. Desai. 1992. Phase transitions in monolayers. *Ann. Rev. Phys. Chem.* 43:207–236.

Lipp, M. M., K. Y. Lee, D. Y. Takamoto, J. A. Zasadzinski, and A. J. Waring. 1998. Coexistence of buckled and flat monolayers. *Phys. Rev. Lett.* 81:1650–1653.

Lipp, M. M., K. Y. Lee, J. A. Zasadzinski, and A. J. Waring. 1997. Design and performance of an integrated fluorescence, polarized fluorescence, and Brewster angle microscope/Langmuir trough assembly for the study of lung surfactant monolayers. *Rev. Sci. Instr.* 68:2574–2582.

McConnell, H. 1991. Structures and transitions in lipid monolayers at the air-water interface. *Annu. Rev. Phys. Chem.* 42:171–195.

McIntyre, R. C., Jr., E. J. Pulido, D. D. Bensard, B. D. Shames, and E. Abraham. 2000. Thirty years of clinical trials in acute respiratory distress syndrome. *Crit. Care Med.* 28:3314–3331.

Mead, J., and C. Collier. 1959. Relation of volume history of lungs to respiratory mechanics in anesthetized dogs. *J. Appl. Physiol.* 14:669–678.

Mizuno, K., M. Ikegami, C. M. Chen, T. Ueda, and A. H. Jobe. 1995. Surfactant protein B supplementation improves in vivo function of a modified natural surfactant. *Pediat. Res.* 37:271–276.

Nakos, G., E. I. Kitsiouli, I. Tsangaris, and M. E. Lekka. 1998. Bronchoalveolar lavage fluid characteristics of early intermediate and late phases of ARDS. Alterations in leukocytes, proteins, PAF and surfactant components. *Intensive Care Med.* 24:296–303.

Notter, R. H. 2000. Lung Surfactants: Basic Science and Clinical Applications. Marcel Dekker, New York.

Peterson, I. R., V. Brzezinski, R. M. Kenn, and R. Steitz. 1992. Equivalent states of amphiphilic lamellae. *Langmuir.* 8:2995–3002.

Pison, U., R. Herold, and S. Schürch. 1996. The pulmonary surfactant system: biological functions, components, physicochemical properties and alterations during lung disease. *Colloid. Surfaces.* 114:165–184.

Robertson, B. 1987. The European multicenter trial of surfactant replacement in neonatal respiratory distress syndrome. *In* International Symposium on Surfactant Replacement Therapy. B. Lachmann, editor. Springer-Verlag, Rotterdam, Netherlands. 123–126.

Schürch, S., J. Goerke, and J. A. Clements. 1976. Direct determination of surface tension in the lung. *Proc. Natl. Acad. Sci. U.S.A.* 73:4698–4702.

Schürch, S., J. Goerke, and J. A. Clements. 1978. Direct determination of volume and time-dependence of alveolar surface tension in excised lungs. *Proc. Natl. Acad. Sci. U.S.A.* 75:3417–3421.

Seeger, W., G. Stöhr, H. R. Wolf, and H. Neuhof. 1985. Alteration of surfactant function due to protein leakage: special interaction with fibrin monomer. *J. Appl. Physiol.* 58:326–338.

Spragg, R. G. 1991. Abnormalities of lung surfactant function in patients with acute lung injury. *In* Adult Respiratory Distress Syndrome. W. M. Zapol and F. Lemaire, editors. Marcel Dekker, New York. 381–395.

Spragg, R. G., P. Richman, N. Gilliard, and T. A. Merritt. 1987. The future for surfactant therapy of the adult respiratory distress syndrome. *In* International Symposium on Surfactant Replacement Therapy. B. Lachmann, editor. Springer-Verlag, Rotterdam, Netherlands. 203–211.

Spragg, R. J., and R. M. Smith. 1998. Surfactant replacement in patients with ARDS: result of clinical trials. *In* Acute Respiratory Distress Syndrome: Cellular and Molecular Mechanisms and Clinical Management. S. Matalon, J. I. Sznajder, and N. A. T. Division, editors. Plenum Press, New York. 107–116.

Taeusch, H. W., K. W. Lu, J. Goerke, and J. A. Clements. 1999. Nonionic polymers reverse inactivation of surfactant by meconium and other substances. *Am. J. Crit. Care Med.* 159:1391–1395.

Tanaka, Y., T. Takei, T. Aiba, K. Masuda, A. Kiuchi, and T. Fujiwara. 1986. Development of synthetic lung surfactants. *J. Lipid Res.* 27:475–485.

Tschumperlin, D. J., and S. S. Margulies. 1999. Alveolar epithelial surface area-volume relationship in isolated rat lungs. *J. Appl. Physiol.* 86:2026–2033.

Wirtz, H. R., and L. G. Dobbs. 2000. The effects of mechanical forces on lung functions. *Respir. Physiol.* 119:1–17.

Yamanaka, T., N. Ogihara, T. Ohhori, H. Hayashi, and T. Muramatsu. 1997. Surface chemical properties of homologs and analogs of lysophosphatidylcholine and lysophosphatidylethanolamine in water. *Chem. Phys. Lipid.* 90:97–107.